

# Loss of Fas Receptor Function Preserves Photoreceptor Structure and Function in Two Mouse Models of Inherited Retinal Degeneration

Jingyu Yao,<sup>1</sup> Tiantian Wang,<sup>1,2</sup> Lin Jia,<sup>1</sup> Yaoyan Qiu,<sup>1,3</sup> and David N. Zacks<sup>1</sup>

<sup>1</sup>Department of Ophthalmology and Visual Sciences, University of Michigan Medical School, Kellogg Eye Center, Ann Arbor, Michigan, United States

<sup>2</sup>Department of Ophthalmology, Xiangya School of Medicine, Xiangya Hospital, Central South University, Changsha, Hunan, China

<sup>3</sup>Department of Ophthalmology, Shanghai Tenth People's Hospital, Tongji University, Shanghai, China

Correspondence: David N. Zacks, University of Michigan, Kellogg Eye Center, 1000 Wall St., Ann Arbor, MI 48103, USA; [davzacks@med.umich.edu](mailto:davzacks@med.umich.edu).

Received: May 18, 2022

Accepted: August 18, 2022

Published: September 9, 2022

Citation: Yao J, Wang T, Jia L, Qiu Y, Zacks DN. Loss of Fas receptor function preserves photoreceptor structure and function in two mouse models of inherited retinal degeneration. *Invest Ophthalmol Vis Sci.* 2022;63(10):5. <https://doi.org/10.1167/iovs.63.10.5>

**PURPOSE.** The genetic heterogeneity of inherited retinal degeneration (IRD) has limited the development of mutation-specific therapies, necessitating the development of therapeutic approaches targeting broadly shared pathophysiologic pathways. The Fas receptor has been reported as a contributor to retinal cell death and inflammation in a wide variety of ocular diseases. The purpose of this study was to assess targeting the Fas pathway as a novel mutation-independent approach to improve photoreceptor survival in IRD.

**METHODS.** We examined the effects of genetic inactivation of the Fas receptor on retinal degeneration in two distinct IRD mouse models, P23H and rd10. The Fas-lpr mouse, which contains a functionally inactive Fas receptor, was crossed with the P23H and rd10 mice to generate P23H/Fas-lpr and rd10/Fas-lpr mice. Fas activation, photoreceptor survival and retinal function were assessed.

**RESULTS.** We detected elevated levels of Fas receptor and microglial activation in the retinas of both P23H and rd10 mice. Inactivation of Fas in these two IRD models (P23H/Fas-lpr and rd10/Fas-lpr mice) resulted in reduced cell death, increased photoreceptor survival, improved retinal function, and reduced microglial activation and inflammatory cytokine production.

**CONCLUSIONS.** The protective effect of a nonfunctional Fas receptor in two different mouse models of retinal degeneration suggests that whereas the individual IRD mutation may be specific, the retina's response to the different stressors appears to be shared and driven by Fas. Reducing Fas activity might represent a potential mutation-independent therapeutic approach to preserve retinal structure and function in patients with IRD.

Keywords: retinal degeneration, apoptosis, Fas, microglia

Inherited retinal degeneration (IRD) is a class of retinal diseases resulting from mutations in nearly 300 different genes. It is a common cause of the blindness, occurring in approximately 1 in 3000 people in the United States. This extreme genetic heterogeneity has limited the development of mutation-specific therapies.<sup>1,2</sup> Although recent approval of voretigene neparvovec (Luxturna) for RPE65-mediated IRD validates the concept of mutation-specific therapies,<sup>3</sup> developing similar treatments for each of the nearly 300 different genes would be costly and time-consuming. Thus, there is a substantial unmet medical need for therapies that target broadly shared pathophysiologic pathways that lead to retinal degeneration.

One potential target to help achieve photoreceptor protection is the cell surface receptor Fas (CD95), an extensively characterized death receptor that is also implicated in propagating the inflammatory microenvironment in retinal diseases.<sup>4-6</sup> Fas receptor activation induces cell death and inflammation in a number of models of ocular diseases,

including retinal detachment,<sup>7-10</sup> age-related macular degeneration (AMD),<sup>11-14</sup> and glaucoma.<sup>6,15</sup> Preventing Fas receptor activation in these models results in retinal protection, both through direct inhibition of death pathway activation and also by limiting the disease-induced inflammatory response.<sup>6,9,11,13-17</sup> These studies suggest that although the specific stressors in each of these diseases are different, the response to stress is common and, importantly, driven by Fas. We hypothesize that similarly, whereas the individual IRD mutation may be different across patients, Fas contributes to the photoreceptor degeneration. Therefore, preventing Fas receptor activity represents a possible mutation-independent therapeutic approach to preserving the retina in patients with IRD.

In this study, we examined the effect of a genetically inactivated Fas receptor on retinal degeneration in two distinct IRD mouse models, the P23H model of autosomal dominant retinitis pigmentosa (adRP) and the rd10 model of autosomal recessive retinitis pigmentosa (arRP). In P23H

adRP, there is a mutation that results in the substitution of proline by histidine at amino acid 23 of the rhodopsin (RHO) protein. This RHO variant is one of the most common forms of IRD in North America.<sup>18–20</sup> This mutation has been well studied,<sup>21–24</sup> and it has been shown that in both the P23H mouse model and the human disease, the amino acid substitution results in RHO protein misfolding, elevated endoplasmic reticulum (ER) stress, and activation apoptosis, necroptosis, and autophagic cell death.<sup>25–36</sup> The rd10 mouse contains a missense mutation in the gene encoding for the cGMP phosphodiesterase 6 (PDE6)  $\beta$  subunit, causing persistent cGMP accumulation, excessive calcium influx, oxidative stress, inflammation, and photoreceptor cell death.<sup>37–40</sup> Patients carrying loss-of-function mutations in the Pde6- $\beta$  gene develop arRP. Approximately 5% of patients with retinitis pigmentosa (RP) have a mutation in the gene coding for PDE6- $\beta$ .<sup>41,42</sup> To prevent Fas receptor activity in the P23H and rd10 mice, we crossed these strains with the Fas-lpr mouse, which contains a structural rearrangement in the Fas receptor gene that prevents its expression.<sup>43</sup>

In this study, we found that there were elevated levels of activation of Fas and microglia in the retinas of both P23H and rd10 mice. Crossing these strains with the Fas-lpr mouse resulted in reduced Fas activation, reduced inflammation, and preservation of photoreceptor structure and function. This observation of the protective effect of Fas receptor inactivation in these two different mouse models of IRD suggests that although the individual IRD mutation may be different, both degenerations can be rescued, at least in part, by targeting Fas receptor activity.

## METHODS

### Animals

All experiments were performed following the Association for Research in Vision and Ophthalmology statement for ethical use of animals and were approved by the University Committee on Use and Care of Animals at University of Michigan. The Rho<sup>P23H/P23H</sup> mice and rd10 mice were crossed with Fas-lpr mice respectively to produce P23H/Fas-lpr mice and rd10/Fas-lpr mice. All the strains were purchased from Jackson lab (strain # 000485 [Fas-lpr], 017628 [P23H], and 004297 [rd10]) and in C57BL/6J genetic background. In all experiments, C57BL/6J mice were used as controls. They are referred to as C57 in the text. For experiments with P23H mice, only those heterozygous for the P23H allele were used, as this represents the more common clinical presentation. All mice used in this study were negative for mutation in the *Crb1*<sup>rd8</sup> gene. Mice were born and housed under standard 12 hours of light: 12 hours of dark in the vivarium of the University of Michigan Kellogg Eye Center. Light condition measured at the cage was set at 300 lux.

### Antibodies

Antibodies Fas (1:100; Santa Cruz, Dallas, TX, USA), GAPDH (Thermo Fisher, AM4300; 1:80000), RHO (4D2, Novus Biologicals, NBP1-48334; 1:2000), m-Opn (Millipore, AB-5405, 1:1000), Iba1 (1:100, Novus Biologicals, NB100-1028, Littleton, CO, USA); and Goat anti-rabbit and anti-mouse secondary antibodies conjugated to horseradish peroxidase are from Dako (P0447 and P0448; 1:2000). Goat anti-mouse Alexa Fluor 488 (1: 1000) and goat anti-rabbit Alex Fluor 546

(1: 1000) secondary antibodies are from Invitrogen (Paisley, UK).

### Histology

The eyes were enucleated after marking the cornea at the 12 o'clock position for orientation then fixed in 4% paraformaldehyde overnight at 4°C before paraffin embedding and 6  $\mu$ m paraffin sections were produced using a microtome (Shandon AS325, Thermo Scientific, Cheshire, England, UK). Hematoxylin (Fisher Scientific, Hercules, CA, USA) and eosin (Fisher Scientific) staining was performed as described previously.<sup>44</sup> Only sections crossing the optic nerve, containing the superior and inferior of the retina were used for staining and images were obtained with a Leica DM6000 microscope (Leica Corp., Wetzlar, Germany).

### Immunofluorescence on Retinal Sections

The cornea was marked for orientation and retinal sections were prepared as described previously.<sup>44</sup> Sections were blocked with 5% goat serum in PBS with 0.1% Triton X-100 (PBST; Sigma-Aldrich) for 1 hour followed by 3 washes with PBST. Sections were incubated with primary antibodies at 4°C overnight. After being washed with PBST, the sections were incubated with secondary antibodies at room temperature for 1 hour. ProLong Gold with DAPI (Invitrogen, P36941) was applied to mount the slides. Only sections crossing the optic nerve, containing the superior and inferior of the retina were used for staining, and images were taken at comparable areas (600  $\mu$ m from the optic nerve in the inferior retina) of the sections with a fixed gain using a confocal microscope (Leica SP5, Leica Corp., Germany). In this study, 10  $\mu$ m sections were used for RHO and m-Opn staining, and 30  $\mu$ m sections were used for Iba1 staining, with 8 mice of each genotype assessed.

### Immunofluorescence on Retinal Whole Mount

Preparation of the retinas was performed as described previously.<sup>16</sup> Retina samples were incubated with Iba1 antibody at 4°C for 48 hours. After being washed, the retinas were incubated with secondary antibodies overnight at 4°C followed by 3 more washes. Retinas were then incubated with DAPI in room temperature for 2 hours and then mounted on glass slide (Fisher Scientific, Pittsburgh, PA, USA) with the ganglion cell layer facing upward. Z-section confocal images of comparable area of the superior and inferior of the retina were taken with Leica SP5 Confocal Microscope (Leica Corp., Wetzlar, Germany;  $n = 8$  for P23H/Fas-lpr and rd10/Fas-lpr;  $n = 7$  for P23H; and  $n = 9$  rd10).

### Terminal Deoxynucleotidyl Transferase dUTP Nick End Labeling Staining

Terminal deoxynucleotidyl transferase dUTP nick end labeling (TUNEL) was performed on 6  $\mu$ m paraffin sections crossing the optic nerve. For P23H/Fas-lpr, P23H and their C57 controls, the eyes were sampled at age P15. For rd10/Fas-lpr, rd10 and C57 controls, eyes were sampled at age P21. TUNEL was performed using DeadEnd Colorimetric TUNEL System (Promega Corporation, Madison, WI, USA) according to the manufacturer's instructions. For samples of P23H

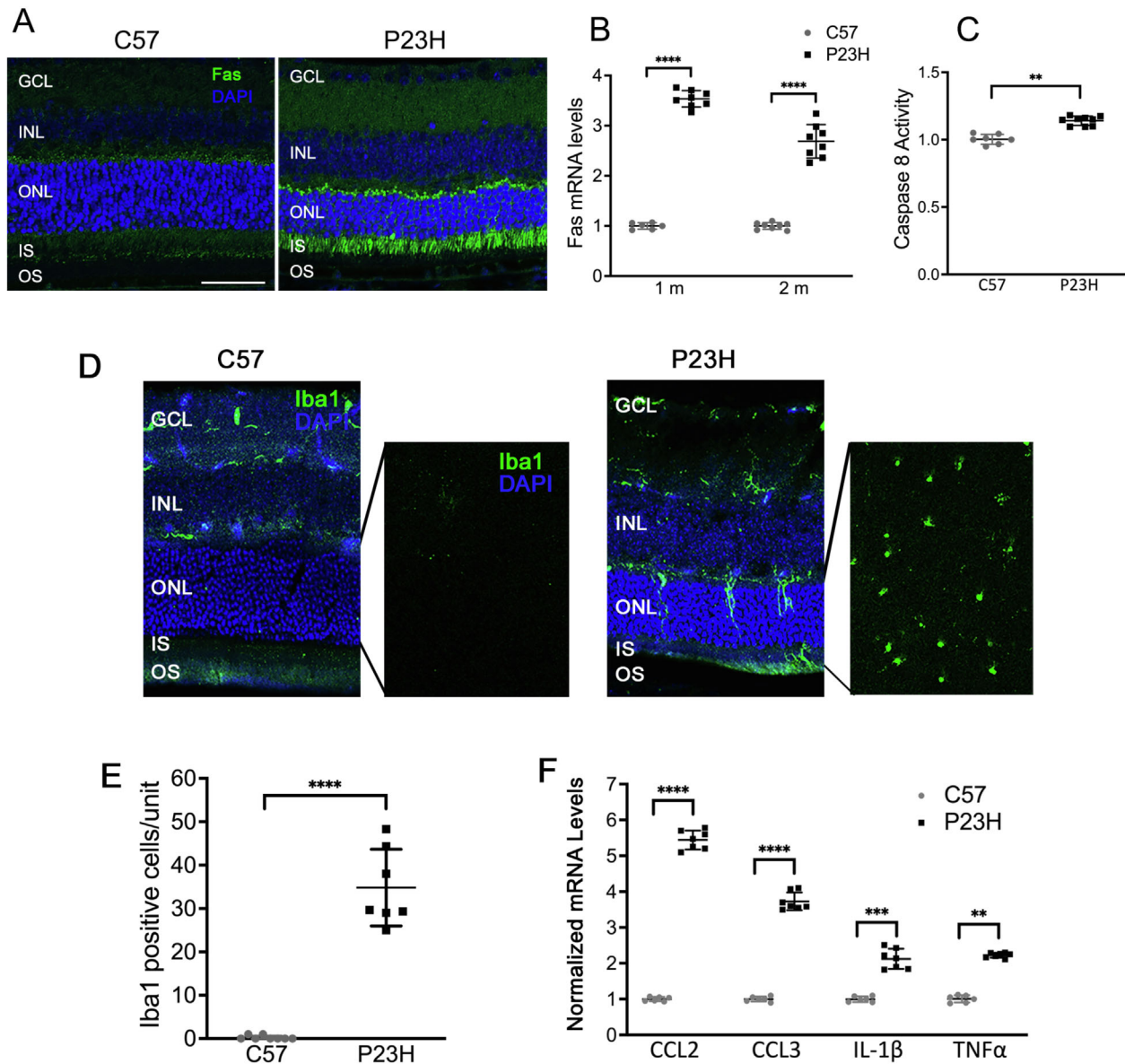


**FIGURE 1.** Activation of Fas-mediated cell death pathway, microglia, and inflammatory cytokines in the retina of the P23H mice. **(A)** Representative Fas (green) staining images for P23H and C57 mice at 1 month of age. Nuclei were counterstained with DAPI (blue). **(B)** Quantification of transcript levels of Fas receptor in the retinas of P23H and C57 mice at 1 and 2 months of age, respectively, normalized to C57 mice. **(C)** Quantification for caspase 8 activity in the retina of P23H and C57 mice at 2 months of age, normalized to C57 mice ( $n = 8$  for P23H; and  $n = 7$  for C57). **(D)** Representative confocal images of Iba1 (green) stained 30  $\mu\text{m}$  retinal sections and retinal whole mount of 2-month-old C57 and P23H mouse, showing Iba-1 positive cells in the photoreceptor layer. Nuclei were counterstained with DAPI. **(E)** Quantification of Iba-1-positive cells in the ONL and subretinal space of the retinal whole mount from C57 and P23H mice. The counting unit is a confocal image at 40 times magnification ( $n = 7$ ). **(F)** Relative mRNA levels of inflammatory cytokines CCL2, CCL3, IL1 $\beta$ , and TNF $\alpha$  in the retinas of P23H at 2 months of age, normalized to C57 mice ( $n = 7$  for P23H; and  $n = 6$  for C57). \*\* $P < 0.01$ ; \*\*\* $P < 0.001$ ; \*\*\*\* $P < 0.0001$ ; unpaired  $t$ -test. Scale bar = 50  $\mu\text{m}$ . GCL, ganglion cell layer; INL, inner nuclear layer; ONL, outer nuclear layer; IS, inner segment; OS, outer segment.

and P23H/Fas-lpr mice, 5 nonoverlapping sections of each sample were used, and images were taken at 20 times magnification for each section. The total number of TUNEL positive photoreceptors of the whole section was counted and averaged for each sample. For samples of rd10 and rd10/Fas-lpr mice, 4 nonoverlapping sections of each mouse were used and 4 images at 40 times magnification were taken at 500 and 1000  $\mu\text{m}$  superiorly and inferiorly from the optic nerve. The number of TUNEL positive photoreceptors in each 40 times magnification images was counted and averaged for

each sample ( $n = 9$  for P23H, P23H/Fas-lpr and rd10;  $n = 8$  for rd10/Fas-lpr; and  $n = 6$  C57).

#### Caspase 8 Activity Assay

Protein preparation for the detection of caspase 8 activity was performed as previously described.<sup>16</sup> Two retinas for each mouse were pooled and homogenized in lysis buffer (20 mM MOPS, pH 7.0, 2 mM EGTA, 5 mM EDTA, 0.1% Triton X-100) containing protease inhibitor (complete

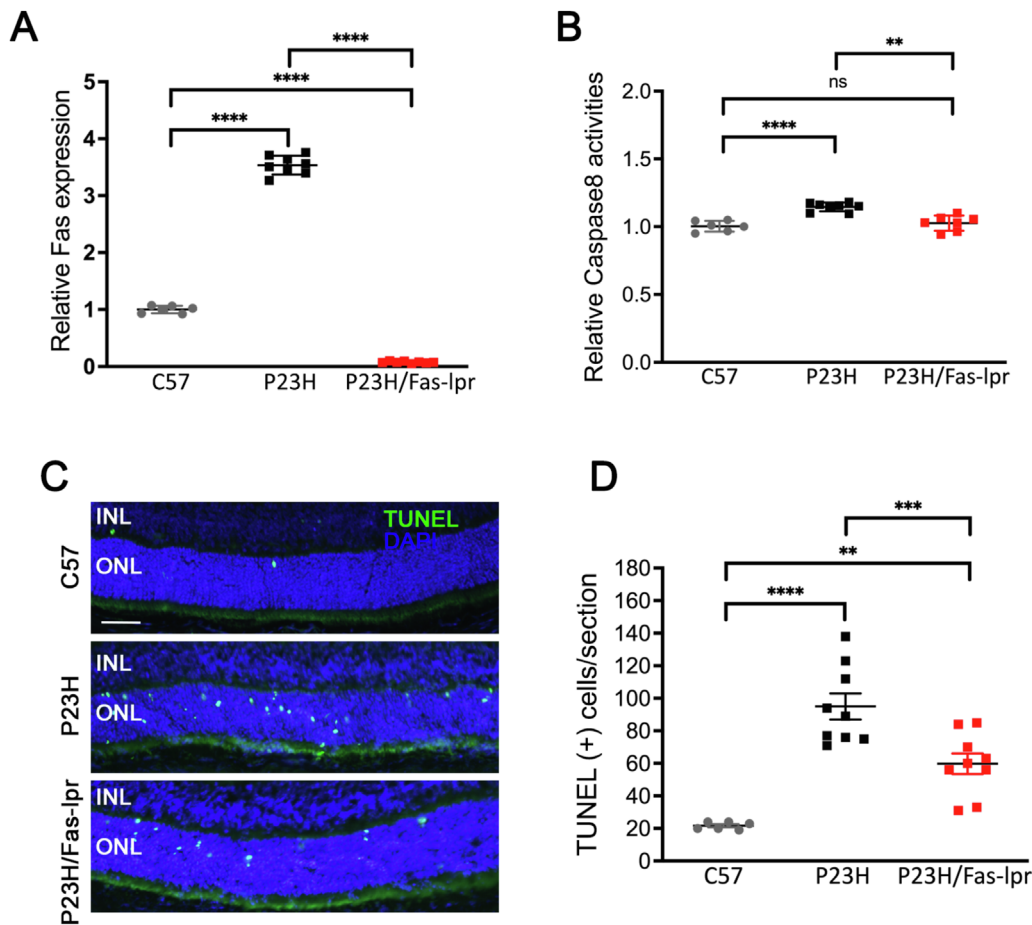


**FIGURE 2.** Decreased photoreceptor cell death in the P23H/Fas-lpr mice. **(A)** Quantification of mRNA levels of Fas in P23H/Fas-lpr, P23H mice at 2 months of age, normalized to C57 mice. **(B)** Quantification for caspase 8 activity in the retina of P23H/Fas-lpr and P23H mice at 2 months of age, normalized to C57 mice ( $n = 8$  for P23H and P23H/Fas-lpr; and  $n = 6$  for C57). **(C)** Representative TUNEL staining images and **(D)** quantification of TUNEL-positive cells in the ONL for P23H/Fas-lpr, P23H, and C57 mice at P15 ( $n = 9$  for P23H and P23H/Fas-lpr; and  $n = 6$  for C57). ns, not significant,  $**P < 0.01$ ;  $***P < 0.001$ ;  $****P < 0.0001$ . One-way ANOVA. Scale bar = 50  $\mu\text{m}$ . GCL, ganglion cell layer; INL, inner nuclear layer; ONL, outer nuclear layer.

protease inhibitor tablet [11697498001; Roche, Indianapolis, IN, USA) and then centrifuged at 10,000  $g$  for 15 minutes at 4°C. Then, 150  $\mu\text{g}$  protein was used for each load and Caspase 8 activity was assayed in duplicate using luminescent Caspase-Glo 8 Assay kit (G8201; Promega, Madison, WI, USA), and luminescence was detected with a plate reader luminometer (Turner Biosystems, Sunnyvale, CA, USA;  $n = 8$  for P23H and P23H/Fas-lpr; and  $n = 6$  for P23H, rd10, rd10/Fas-lpr, and C57).

### Real-Time Polymerase Chain Reaction

A purification kit (Qiagen, 74104) was used for isolation of RNA from one retina of each mouse ( $n = 8$  for P23H/Fas-lpr and rd10/Fas-lpr; and  $n = 6$  for P23H, rd10, and C57). Then, 500 ng of total RNA was converted into cDNA with the SuperScript III Reverse Transcriptionase Kit (18080093; Thermo Fisher Scientific). Transcript levels were assayed in triplicate using a thermal cycler (Bio-Rad CFX96 Real Time System, C1000 Touch Thermal Cycler; Bio-Rad Laboratories, Hercules, CA, USA). Target gene expression levels were normalized to the level of *Rpl19* using a comparative Ct method. Specific primers were as follows: *Fas* (forward 5'-ATGAGATCGAGACAACAGC-

3', reverse 5'-TTAAAGCTTGACACGCACCA-3'); *Caspase 8* (forward 5'-ATGGCGAACTGTGTGACTCG-3', reverse 5'-GTCACCGTGGGATAGGATACAGCA-3'); and *Rpl19* (forward 5'-ATGCCAACTCCCGTCAGCAG-3'; reverse 5'-TCATCCTTCTCATCCAGGTCACC-3'). *Ccl2* (forward 5'-CGTAACTGCATCTGGCTGA-3', reverse 5'-AGCACCAGC-CAACTCTCACT-3'); *Il-1 $\beta$*  (forward 5'-GCCCATCCTC-TGTGACTCAT-3', reverse 5'-AGGCCACAGGTATTTTGTGCG-3'); *Tnfa* (forward 5'-CGTCAGCCGATTGTCTATCT-3', reverse 5'-CGGACTCCGCAAAGT CTAAG-3'); and *Ccl3* (forward 5'-CCTTGCTGTTCTTCTCTG TACC-3'; reverse 5'-CGATGAATTGGCGTGGAATC-3'). The PCR cycling conditions consisted of an initial denaturation of 95°C for 10 minutes followed by 40 cycles of 95°C for 15 to 30 seconds and 60°C for 1 minute.

### Optical Coherence Tomography

Optical coherence tomography (OCT) was performed as described previously<sup>28</sup> using the spectral domain OCT system from BiopTigen, Inc. (Durham, NC, USA). The thickness of the outer nuclear layer (ONL) was measured at 250 and 500  $\mu\text{m}$  superiorly and inferiorly from the optic nerve for P23H and P23H/Fas-lpr; and measured at 500  $\mu\text{m}$  from the

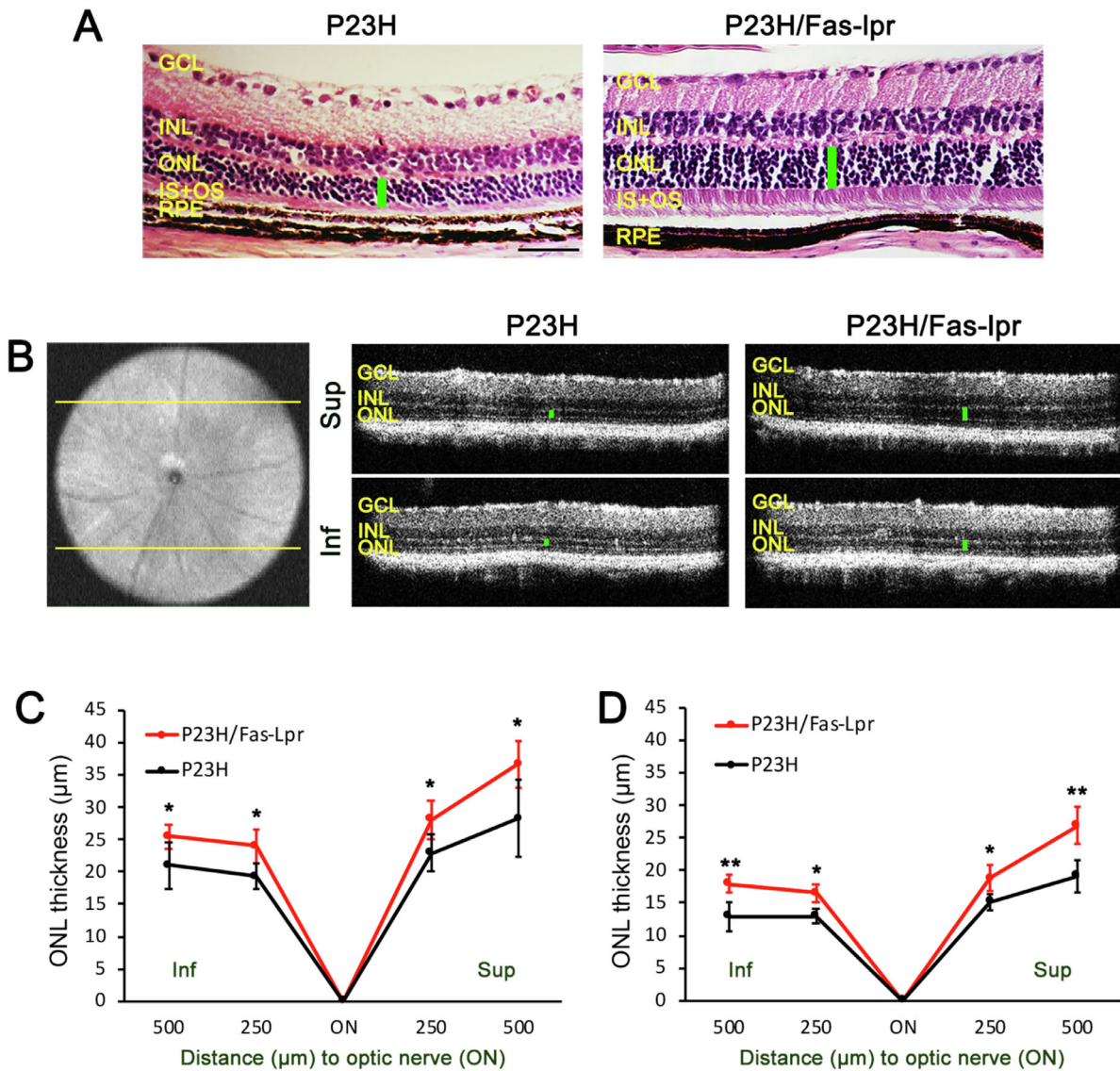


**FIGURE 3.** Increased photoreceptor survival in P23H/Fas-lpr mouse retina compared with P23H controls. (A) Representative H&E staining images show preserved photoreceptors in the retina of P23H/Fas-lpr mice at 4 months of age. (B) Representative optical coherence tomography (OCT) images of superior (sup) and inferior (inf) retina of 4-month-old P23H/Fas-lpr and P23H control. (C) Quantification of the thickness of the ONL (indicated by green bars in the OCT images) of the superior and inferior retina measured at both 250 and 500 µm from the optic nerve head by OCT in P23H/Fas-lpr, and P23H mice at the age of 4, and (D) 6 months. Scale bar = 50 µm (*n* = 19 for P23H/Fas-lpr, and *n* = 20 for P23H). \**P* < 0.05; \*\**P* < 0.01; unpaired *t*-test. GCL, ganglion cell layer; H&E, hematoxylin-eosin; INL, inner nuclear layer; ONL, outer nuclear layer; RPE, retinal pigment epithelium.

optic nerve at superior, inferior, temporal, and nasal areas of the retina (*n* = 19 for P23H/Fas-lpr, *n* = 20 for P23H, *n* = 18 for rd10/Fas-lpr; and *n* = 13 for rd10).

**Electroretinography**

Electroretinography (ERG) was performed using the Espion e2 recording system (Diagnosys, Lowell, MA, USA) as previously described.<sup>28</sup> After overnight dark adaptation, scotopic ERG was recorded at 0.01, 10, and 32 log cd s/m<sup>2</sup>. After 10 minutes of light-adaptation, photopic function was assessed at 10, 32, and 100 log cd s/m<sup>2</sup>. The amplitudes were measured using Espion V6 software (Diagnosys, Lowell, MA,

USA *n* = 18 for P23H and P23H/Fas-lpr, *n* = 23 for rd10/Fas-lpr; *n* = 20 for rd10, and *n* = 10 for C57).

**Statistical Analysis**

Unpaired *t*-test was used for comparisons between two groups, and 1-way ANOVA was used for comparisons across more than 2 groups followed by Tukey multiple comparison test. Prism (GraphPad, Inc., La Jolla, CA, USA) and Microsoft Office Excel (Richmond, WA, USA) were used for statistical analysis and graphing. Results were expressed as mean ± standard deviation. Differences were considered significant at *P* < 0.05.

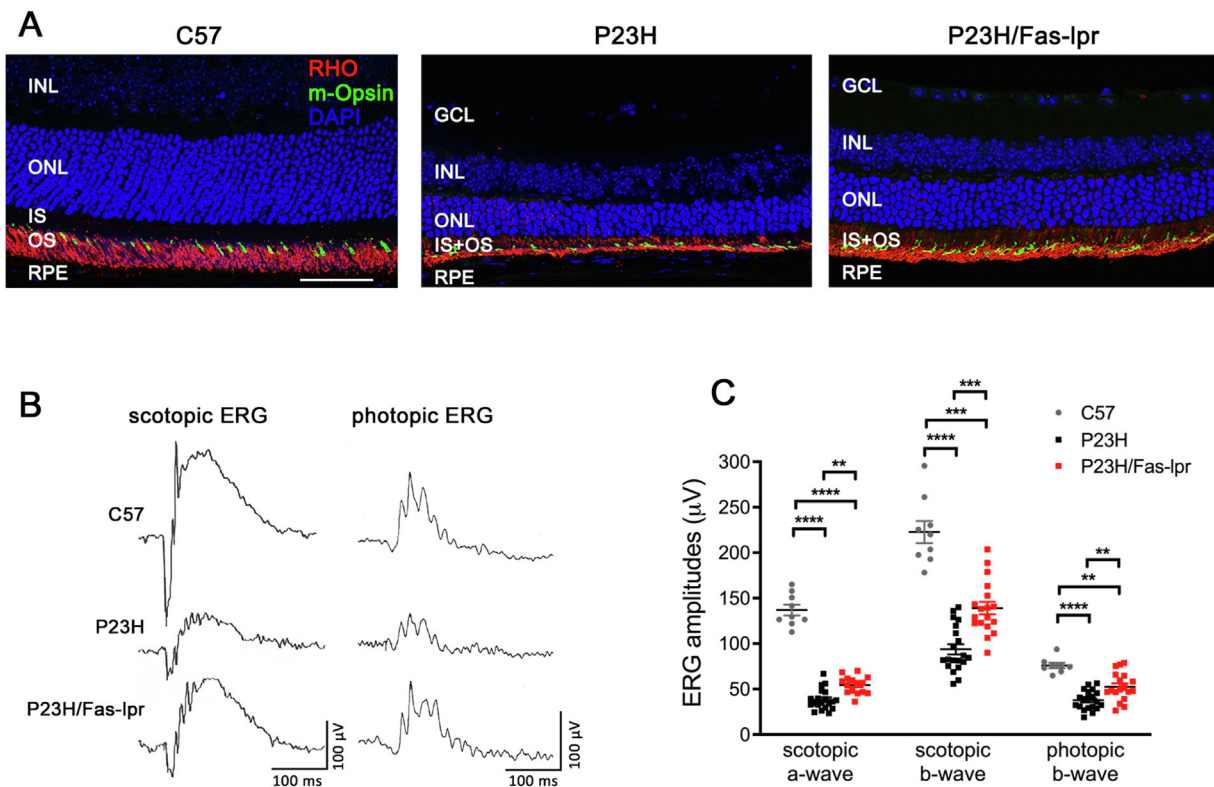


**FIGURE 4.** Preserved retinal function in P23H/Fas-lpr mice. **(A)** Representative immunostaining images of inferior retina of four-month-old P23H/Fas-lpr, P23H and C57 mice, stained with rhodopsin (RHO in red), m-opsin (green), and DAPI (blue). **(B)** Representative scotopic (at 10 cd s/m<sup>2</sup>) and photopic (at 100 cd s/m<sup>2</sup>) ERG at 4 months of age in P23H/Fas-lpr, P23H, and C57 mice at 4 months of age. **(C)** Quantification of amplitudes of scotopic a-wave, scotopic b-wave, and photopic b-wave confirms the preservation in retinal function ( $n = 23$  for rd10/Fas-lpr;  $n = 20$  for rd10, and  $n = 10$  for C57). Scale bar = 50 µm. \* $P < 0.01$ ; \*\* $P < 0.001$ ; \*\*\* $P < 0.0001$ ; \*\*\*\* $P < 0.00001$ ; 1-way ANOVA. INL, inner nuclear layer; ONL, outer nuclear layer; IS, inner segment; OS, outer segment.

## RESULTS

### Fas Activation and Inflammation in the P23H Retina

We first assessed whether Fas was activated in the P23H mouse retina. By 1 month of age, Fas expression was increased in the photoreceptors, as demonstrated by increased Fas staining in retinal sections of P23H mice compared to the control mice (Fig. 1A). Fas transcript levels increased approximately 3.5 and 3 folds in the retinas of 1 month and 2 months old P23H mice, respectively, as compared to the retinas from age-matched C57 controls (Fig. 1B). Caspase 8 is considered as the first downstream target of the activated Fas receptor and a hallmark of Fas activation. Caspase 8 activity was increased approximately 15% in the retinas of P23H mice compared with C57 controls (Fig. 1C).

Previous work has demonstrated that an inflammatory microenvironment plays a role in retinal disease progression, and that this is often manifested by the expression of inflammatory cytokines,<sup>6–15</sup> which serve to activate and recruit microglia, macrophages, and other immune cells to the retina. To detect immune cells in the retina, we stained for Iba1 on both retinal whole mounts and cross sections. We detected activation of Iba-1 positive cells and their migration into the ONL in the P23H mice but not the C57 mouse retinas, where the Iba1-positive cells were in their quies-

cent state and localized in the inner retina (Figs. 1D, 1E). Transcript levels of inflammatory cytokines including CCL2, CCL3, IL-1 $\beta$ , and TNF $\alpha$  were elevated in the retinas of P23H mice as compared to C57 controls (Fig. 1F). These data demonstrate elevated Fas activity and inflammation in the outer retina of the P23H mice.

### Loss of Fas Activity Protects Photoreceptor Cell Viability and Function in the P23H Retina

To examine the potential protective effect of Fas-receptor inhibition on retinal degeneration, P23H mice were crossed with Fas-lpr mice, which possess a mutation in Fas that renders the Fas-receptor inactive, to generate P23H/Fas-lpr mice. Fas transcript levels in the retinas of P23H/Fas-lpr mice confirmed the efficient suppression of Fas expression (Fig. 2A). Retinas from the P23H/Fas-lpr and control mice were analyzed for markers of apoptosis. Caspase 8 activity in the P23H/Fas-lpr mice (Fig. 2B) was lower as compared with P23H controls, consistent with decreased Fas activation. TUNEL labeling was performed on retinal sections from mice at P15, the time point that has been shown to be the peak of TUNEL positive cells in the P23H mouse retina.<sup>29</sup> The P23H mice had a significantly higher number of cells undergoing apoptosis, as indicated by TUNEL staining in the ONL compared to the C57 control, whereas Fas deficient P23H/Fas-lpr mice showed significant reduction in the

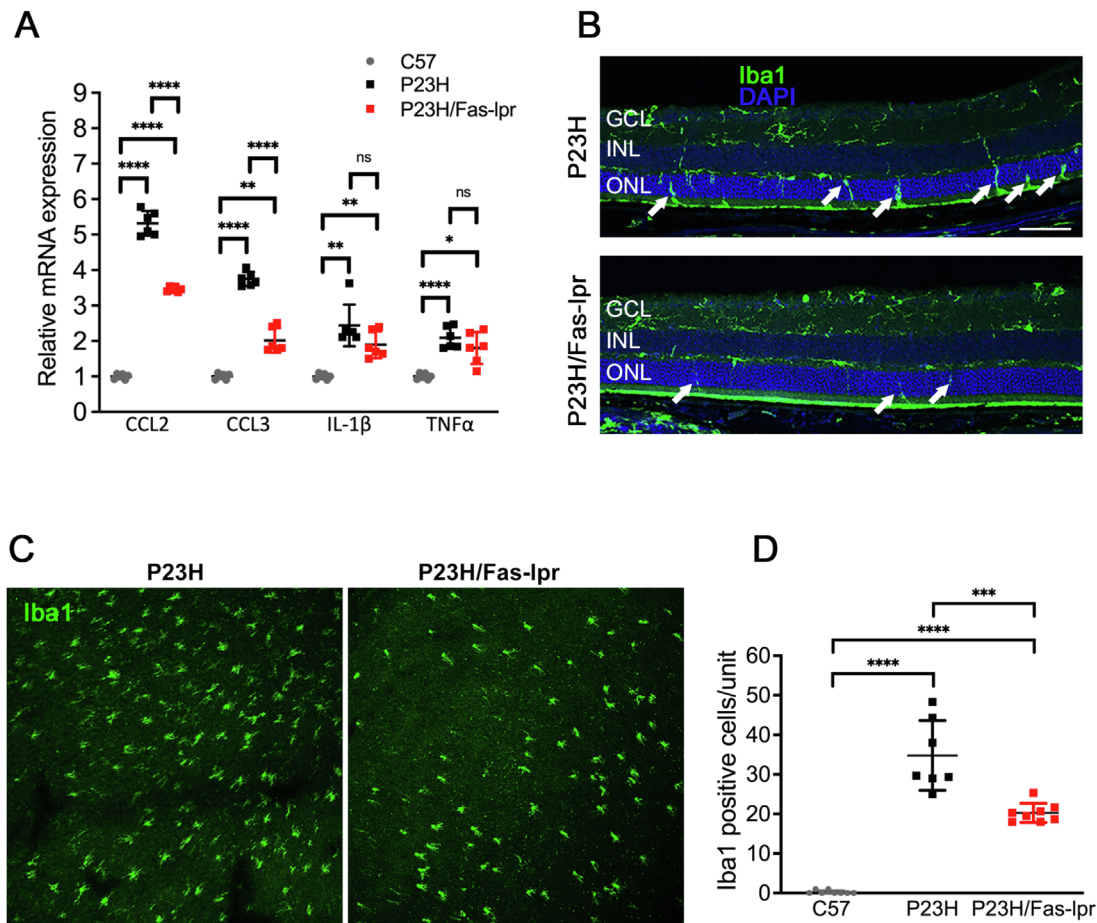


**FIGURE 5.** Reduced inflammation in the P23H/Fas-lpr mouse retina. **(A)** Relative mRNA levels of inflammatory cytokines CCL2, CCL3, IL1 $\beta$ , and TNF $\alpha$  in retinas of P23H/Fas-lpr, P23H, and C57 mice at two months of age, normalized to levels in the wild-type C57 mice ( $n = 6$ ). **(B)** Representative immunostaining images of retinal sections from inferior retinas of P23H and P23H/Fas-lpr mice at 2 months of age stained with Iba-1 and DAPI. White arrows indicate Iba1-positive cells resented in the ONL of the retina. **(C)** Representative images for ONL from inferior area of the retinal whole mount of P23H/Fas-lpr and P23H mice stained with Iba1 at 2 months of age. **(D)** Quantification of Iba1-positive cells in the ONL and subretinal space of the inferior retina of P23H and P23H/Fas-lpr mice ( $n = 8$  for P23H/Fas-lpr; and  $n = 7$  for P23H and C57). ns, not significant; \* $P < 0.05$ ; \*\* $P < 0.01$ ; \*\*\* $P < 0.001$ ; \*\*\*\* $P < 0.0001$ ; 1-way ANOVA. GCL, ganglion cell layer, INL, inner nuclear layer, ONL, outer nuclear layer; Scale bar = 100  $\mu$ m.

amount of TUNEL positive cells as compared to the P23H control mice, although not down to the level of the C57 retina (Figs. 2C, 2D).

Histological analysis of retinal samples at 4 months showed a significant thinning of the ONL in the P23H retina, whereas the Fas-deficient P23H/Fas-lpr mice maintained a thicker ONL (Fig. 3A). In P23H mice, the rate of photoreceptor loss is greater in the inferior retina as compared to the superior retina.<sup>34</sup> The thickness of the ONL, where the photoreceptor cell nuclei reside, was measured in vivo using OCT in both the superior and inferior portions of the retina (Fig. 3B). Fas deficiency resulted in preservation of ONL thickness in both the superior and inferior retina in the P23H/Fas-Lpr mice compared with P23H controls at 4 months and 6 months of the age (Figs. 3C, 3D).

The retinas of the P23H mice have shorter outer segments and reduced staining for rhodopsin and cone m-opsin as compared to control mice, and this was improved in the P23H/Fas-lpr mouse retina (Fig. 4A). The visual function of P23H/Fas-lpr mice and control P23H mice was analyzed by measuring the electroretinogram at age 4 months. Both scotopic and photopic responses of P23H/Fas-lpr mice

were significantly higher than their age-matched P23H controls, although lower than the ERG response of C57 mice (Figs. 4B, 4C).

### Fas Deficiency Reduced Immune Cell Activation and Cytokine Production in the P23H Retina

To assess the effects of deficient Fas signaling on immune activation in P23H mice, retina samples of P23H/Fas-lpr, control P23H, and wild type C57 mice were collected to perform immunostaining and real-time PCR (RT-PCR). Transcript levels of CCL2 and CCL3 were significantly reduced in the retinas of P23H/Fas-lpr mice compared with P23H controls, and levels of IL-1 $\beta$  and TNF $\alpha$  trending slightly downward (Fig. 5A). Furthermore, as compared to P23H controls, significantly fewer Iba1-positive cells were present in the ONL of the P23H/Fas-lpr mice (Fig. 5B) and retinal whole mount (Figs. 5C, 5D). These findings support the conclusion that Fas-inhibition reduced cytokine production and decreased immune cell activation and migration in P23H retinas.

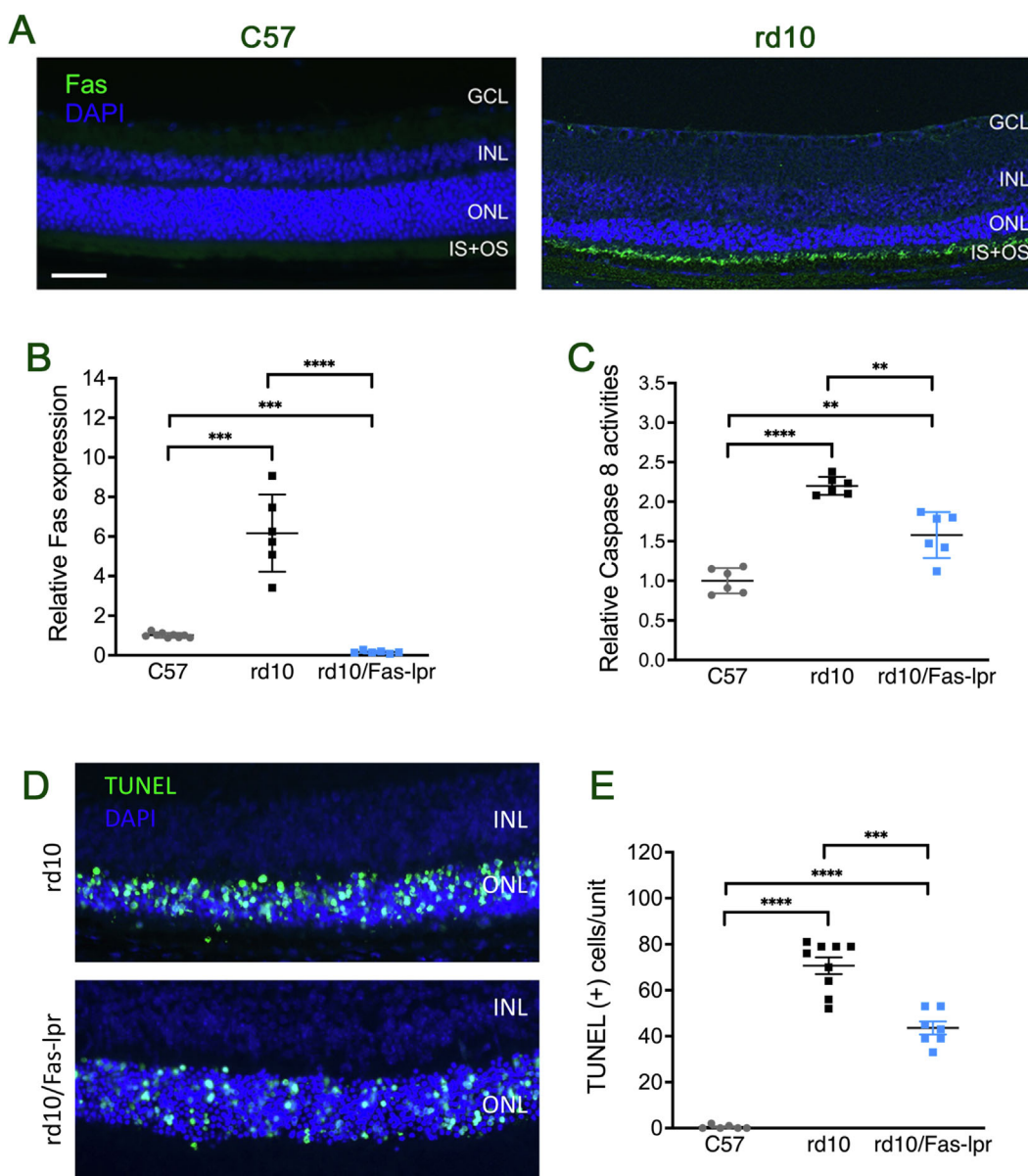


**FIGURE 6.** Reduced Fas-mediated photoreceptor cell death in the rd10/Fas-lpr mice. **(A)** Representative Fas (green) and DAPI (blue) staining images for rd10 and C57 mice at P21 showing activation of Fas-mediated cell death pathway in the retina of the rd10 mice. **(B)** Quantification of mRNA levels of Fas in rd10/Fas-lpr, rd10 mice at P21, normalized to C57 mice. **(C)** Quantification for caspase 8 activity in the retina of rd10/Fas-lpr and rd10 mice at P21, normalized to C57 mice ( $n = 6$ ). **(D)** Representative TUNEL staining images and **(E)** quantification of TUNEL-positive cells in the ONL for rd10/Fas-lpr, P23H and C57 mice at P21 ( $n = 6$  for rd10/Fas-lpr and c57; and  $n = 9$  for rd10). \*\* $P < 0.01$ ; \*\*\* $P < 0.001$ ; \*\*\*\* $P < 0.0001$ ; 1-way ANOVA. Scale bar = 50  $\mu\text{m}$ . GCL, ganglion cell layer; INL, inner nuclear layer; ONL, outer nuclear layer; IS, inner segment; OS, outer segment.

### Loss of Fas Activity Protects Photoreceptor Cell Viability and Function in the rd10 Retina

The rd10 retina appears nearly normal for the first 2 weeks of life but it then rapidly loses photoreceptors by 5 to 6 weeks of age.<sup>45–47</sup> The peak of the photoreceptor death occurs at approximately P21.<sup>47</sup> We performed immunostaining for Fas at this time point and found increased Fas staining in the photoreceptors of rd10 mice as compared to C57 control mice (Fig. 6A). Transcript levels of Fas also increased significantly in retinas of 3 week and 4 week old rd10 mice, respectively, as compared to age-matched C57 controls (Fig. 6B).

Caspase 8 activity at 3 weeks was doubled in the rd10 retina as compared to the C57 controls (Fig. 6C).

We crossed the rd10 mice with Fas-lpr mice to generate the rd10/Fas-lpr mouse strain. As in the case of the P23H/Fas-lpr strain, the Fas transcript level in the retinas of rd10/Fas-lpr mice was suppressed, confirming the efficient inhibition of Fas-receptor expression (see Fig. 6B). There were also lower levels of caspase 8 activity in the rd10/Fas-lpr mice compared with rd10 controls (see Fig. 6C). Decreased number of TUNEL positive photoreceptors was also observed in the retinas of rd10/Fas-lpr mice at 3 weeks of age (Figs. 6D, 6E).

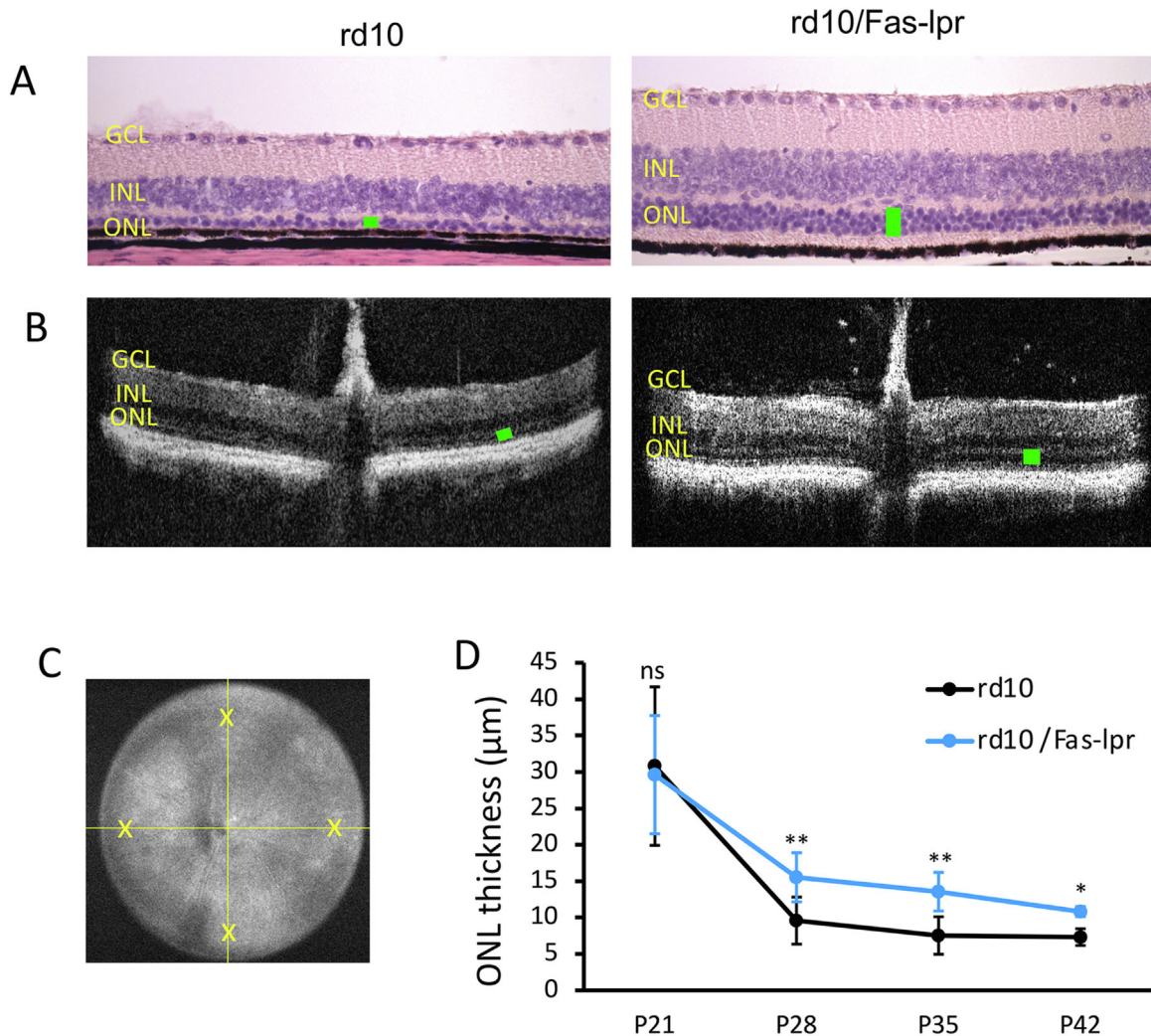


**FIGURE 7.** Increased photoreceptor survival in rd10/Fas-lpr mouse retina compared with rd10 controls. (A) Representative H&E staining images show preserved photoreceptors in the retina of rd10/Fas-lpr mice at P28. (B) Representative optical coherence tomography (OCT) images of superior (sup) and inferior (inf) retina of rd10/Fas-lpr and rd10 control at P28 (green bars indicate ONL). (C) Yellow “x” on the fundus photograph demonstrates that ONL thickness were measured at 500  $\mu\text{m}$  from the optic nerve at superior, inferior, temporal, and nasal areas of the retina, then averaged for each mouse. (D) Quantification of the thickness of the ONL of retina measured at 500  $\mu\text{m}$  from the optic nerve head by OCT in rd10/Fas-lpr, and rd10 mice at P21, P28, P35, and P42 ( $n = 13$  for rd10; and  $n = 18$  for rd10/Fas-lpr),  $*P < 0.05$ ;  $**P < 0.01$ . ns, not significant. Unpaired  $t$ -test. GCL, ganglion cell layer; H&E, hematoxylin-eosin; INL, inner nuclear layer; ONL, outer nuclear layer; RPE, retinal pigment epithelium.

By the age of 5 weeks, there is only a single layer of photoreceptors left in the rd10 retina. In contrast, the ONL of rd10/Fas-lpr contained 3 to 4 layers of photoreceptors (Fig. 7A). We also measured the thickness of the ONL measured by OCT, and this confirmed the thicker ONL in the retinas of rd10/Fas-lpr mice (Figs. 7B–D). Immunostaining showed increased staining for rhodopsin and cone opsin in the retinas of rd10/Fas-lpr mice (Fig. 8A). Consistent with the increased production of opsin, both scotopic and photopic ERGs of rd10/Fas-lpr mice were significantly higher than their age-matched rd10 controls (Figs. 8B, 8C). These results indicate that Fas inhibition helped preserve photoreceptor survival and visual function in the rd10 mice, as it did in the P23H mice.

### Fas Deficiency Reduced Immune Cell Activation and Cytokine Production in the rd10 Retina

Studies have demonstrated increase inflammation in the rd10 retina,<sup>48–50</sup> and we also detected significantly elevated transcript levels for CCL2, CCL3, IL-1 $\beta$ , and TNF $\alpha$  in the retinas of these mice. In the retinas of rd10/Fas-lpr mice, however, levels of these inflammatory cytokines are markedly reduced (Fig. 9A). Iba1 staining on both retinal sections (Fig. 9B) and retinal whole mount (Figs. 9C, 9D) revealed significantly fewer immune cells in the ONL of the P23H/Fas-lpr mice. These results suggest that Fas-inhibition reduced cytokine production and microglia activation in the rd10 retinas.

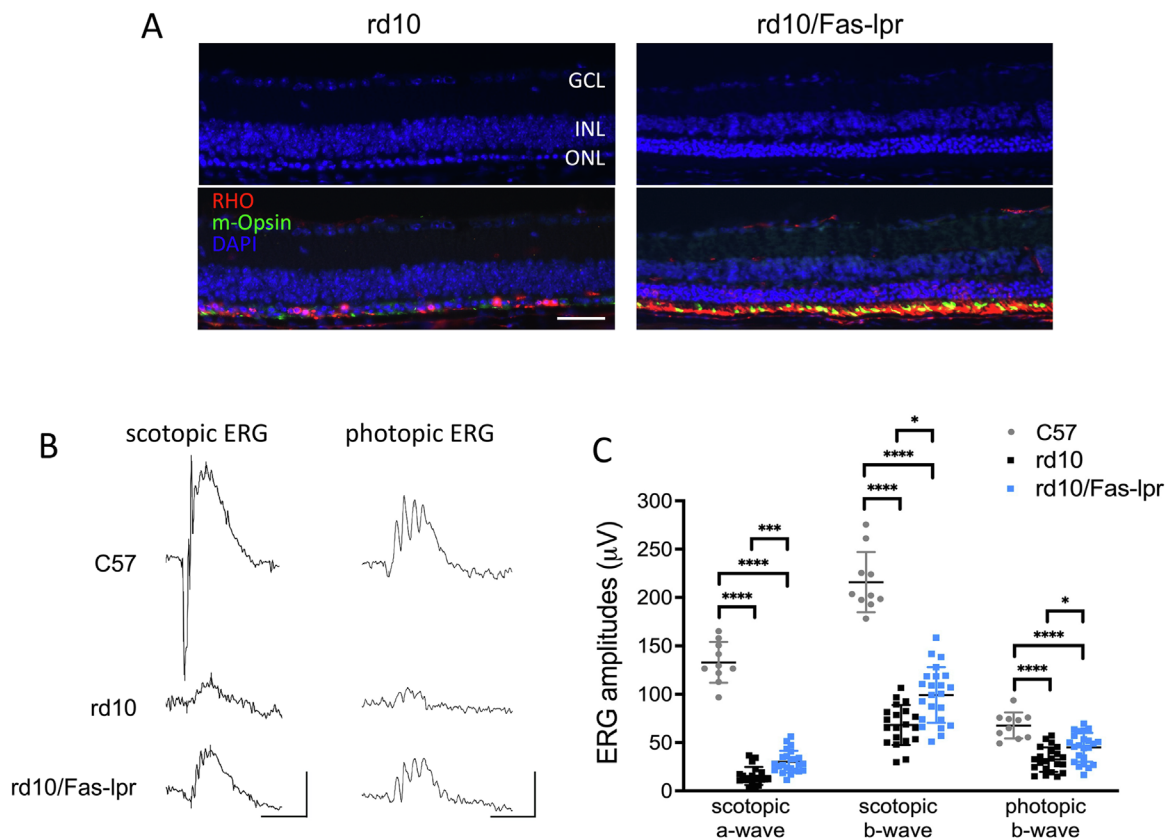


**FIGURE 8.** Improved retinal function in rd10/Fas-lpr mice. **(A)** Representative immunostaining images of inferior retina of rd10/Fas-lpr, rd10 and C57 mice at P28, stained with rhodopsin (RHO in red), m-opsin (green), and DAPI (blue). **(B)** Representative scotopic (at 10 cd s/m<sup>2</sup>) and photopic (at 100 cd s/m<sup>2</sup>) ERG traces of rd10/Fas-lpr, rd10 and C57 mice at P28. **(C)** Quantification of amplitudes of scotopic a-wave, scotopic b-wave, and photopic b-wave. Scale bar = 50 µm. \**P* < 0.05; \*\*\**P* < 0.001; \*\*\*\**P* < 0.0001, 1-way ANOVA. GCL, ganglion cell layer; INL, inner nuclear layer, ONL, outer nuclear layer.

## DISCUSSION

Although not required for normal retinal development,<sup>51</sup> the Fas pathway has been previously shown to contribute to outer retinal degeneration in a number of diseases, including retinal detachment, AMD, and glaucoma. In all these cases, despite the heterogeneity in inciting stressor leading to photoreceptor death, be it retina-RPE separation (retinal detachment), oxidative stress (AMD), or elevated intraocular pressure (glaucoma), there is an upregulation and activation of the Fas pathway that results in death pathway activation as well as an increase in the intra-retinal inflammation. In animal models of these diseases, genetic or pharmacologic inhibition of Fas activation greatly reduces cell death and inflammation. Recently, three clinical trials have been initiated in these conditions, exploring the potential of Fas inhibition to improve visual outcomes in patients with these diseases (clinicaltrials.gov identifier: NCT03780972, NCT04744662, and NCT05160805).

For patients with IRD, there exists a large unmet need for therapies that preserve retinal structure and function. Analogous to the heterogeneity in disease etiology for retinal detachment, AMD, and glaucoma, in IRD there is heterogeneity in the underlying genetic defect, making specific therapies for all causative mutations an extremely challenging proposition. Our data suggest that regardless of the heterogeneity in causative mutations, the Fas path-

way becomes upregulated and activated. As in the other disease states, the activation of the Fas pathway in IRD is combined with activation of an inflammatory response. By targeting this core, common pathophysiologic pathway that contributes to the degeneration, there is potential to provide mutation-independent therapy to prolong the survival and improve the function of the retinal cells. Our data demonstrate that reduced Fas signaling in two independent models of IRD reduces photoreceptor cell death and intra-retinal inflammation and improves retinal function.

The absence of Fas signaling that results from the crossing of the IRD mouse strain to the *lpr* strain results in two major effects. First, is the reduction in pro-death pathway activation. In both the P23H and rd10 models of IRD, crossing with the *lpr* mouse strain resulted in reduced caspase 8 activity and reduced entrance of the cell into the apoptotic cascade, as evidenced by reduced TUNEL-positive staining. Cleavage of caspase 8 is the first downstream effect of an activated Fas receptor. Preventing Fas function prevents the cleavage of caspase 8 and the subsequent activation of the apoptotic cascade. This is similar to what is seen in the other models of retinal disease mentioned above when Fas signaling is inhibited.

A second major consequence of the reduced Fas activity in these IRD models is the reduction in the activation of microglia and macrophages, as demonstrated by the reduction in Iba1-positive cells in the P23H/Fas-*lpr* and

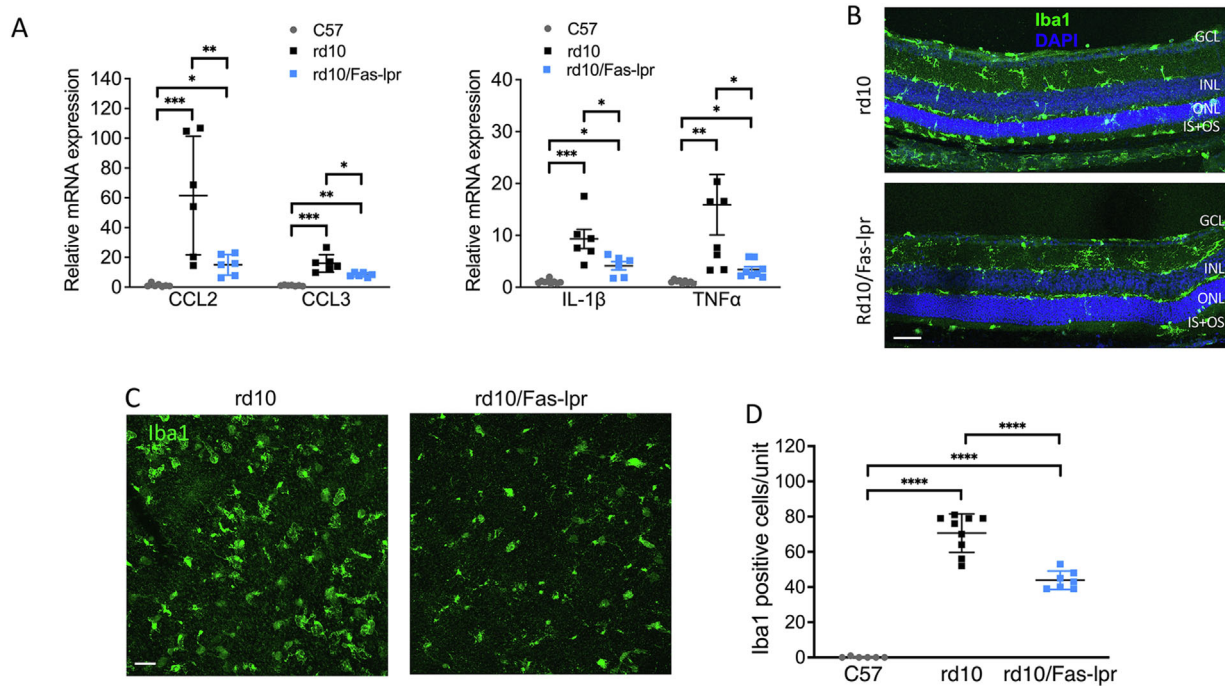


**FIGURE 9.** Decreased inflammation in the rd10/Fas-lpr mouse retina. (A) Relative mRNA levels of inflammatory cytokines CCL2, CCL3, IL1 $\beta$ , and TNF $\alpha$  in retinas of rd10/Fas-lpr, rd10 and C57 mice at P21, normalized to C57 mice ( $n = 6$ ). (B) Representative immunostaining images of retinal sections of rd10/Fas-lpr, and rd10 mice at P21 stained with Iba-1 and DAPI. (C) Representative images for ONL from retinal whole mount of rd10/Fas-lpr and rd10 mice stained with Iba1 at P21. (D) Quantification of Iba1-positive cells in the ONL and subretinal space of the rd10/Fas-lpr, rd10 and C57 mice ( $n = 7$  for rd10/Fas-lpr;  $n = 9$  for rd10; and  $n = 6$  for C57). \* $P < 0.05$ ; \*\* $P < 0.01$ ; \*\*\* $P < 0.001$ ; \*\*\*\* $P < 0.0001$ , 1-way ANOVA. GCL, ganglion cell layer; INL, inner nuclear layer; ONL, outer nuclear layer; IS, inner segment; OS, outer segment. Scale bar = 50  $\mu\text{m}$ .

rd10/Fas-lpr strains. Activation of microglia and macrophages is well demonstrated in mouse models of IRD,<sup>52–56</sup> and is thought to contribute to the degeneration of the retina. By reducing Fas activity, there is reduced activation of these cells, which may be contributing to protection. Additionally, we observed a reduction in various molecular markers of inflammation. The chemokine CCL2 is important for macrophage recruitment, and was reduced in the Fas-lpr crosses. We also observed reduced CCL3, also known as macrophage inflammatory protein (MIP)-1 alpha, in the Fas-lpr cross strains. Reduced CCL3 has been previously correlated with increased photoreceptor survival in IRD. Reducing Fas receptor activity is a potential method for reducing the levels of this chemokine to obtain this protective effect. Although the reduction in interleukin (IL)-1 $\beta$  and tumor necrosis factor (TNF)-alpha did not reach statistical significance in the P23H/Fas-lpr mouse, it did in the rd10/Fas-lpr mouse. Both these proteins are associated with the activation of apoptosis, and their reduction is consistent with the protective effect observed.

A major limitation observed in our results is that the protection conferred by the inactive Fas receptor is only partial, and the retina still continues to degenerate albeit at a slower rate. This is very different from the published literature on reduced Fas signaling in animal models of retinal detachment,<sup>4</sup> AMD,<sup>16</sup> and glaucoma,<sup>15</sup> where the protective effect is much greater. Although activation of Fas occurs in all these disease models, the stressors involved in IRD are intrinsic to the cell (i.e. a genetic mutation), whereas in the other disease states the stressor is externally imposed upon

an otherwise normal photoreceptor cell. Lack of Fas activity may be sufficient to prevent cell death in the other diseases, but appears to be only partially protective in the IRD models tested here, as evidenced by the OCT and ERG data. Which other death pathways are responsible for the continued cell death remains an area of active investigation. Regardless, our data show that even the moderate protection afforded by inactivation of Fas translates into improved retinal function in the as seen on the electroretinogram.

In summary, our data show that reduced Fas receptor activity results in reduced death pathway activation and inflammation in the retina of two mouse models of inherited retinal degeneration. This approach targeted a common pathophysiologic mechanism underlying the death of the retinal cells without addressing the underlying genetic defect itself. It remains to be seen how this translates in terms of efficacy in patients with IRD, and Fas inactivation may need to be part of a multi-therapy approach to target various pathways that contribute to the retinal degeneration. Even if incomplete, the rescue afforded by reducing Fas activity may be significant to a patient suffering from one of these degenerations and further work should be conducted to explore this potential.

### Acknowledgments

Supported by the National Eye Institute (EY-020823 to D.N.Z., and Core Center EY007003 to University of Michigan Kellogg Eye Center), Research Prevent Blindness, Inc. (to D.N.Z.), Foundation Fighting Blindness (to D.N.Z.).

**Disclosure:** J. Yao, None; T. Wang, None; L. Jia, None; Y. Qiu, None; D.N. Zacks, None

## References

- RetNet – Retinal Information Network. Accessed November 30, 2018. Available at: <https://sph.uth.edu/retnet/>.
- Sohocki MM, Daiger SP, Bowne SJ, et al. Prevalence of mutations causing retinitis pigmentosa and other inherited retinopathies. *Hum Mutat.* 2001;17(1):42–51.
- Miraldi Utz V, Coussa RG, Antaki F, Traboulsi EI. Gene therapy for RPE65-related retinal disease. *Ophthalmic Genet.* 2018;39(6):671–677.
- Zacks DN, Boehlke C, Richards AL, Zheng QD. Role of the Fas-signaling pathway in photoreceptor neuroprotection. *Arch Ophthalmol.* 2007;125:1389–1395.
- Chinskey ND, Besirli CG, Zacks DN. Retinal cell death and current strategies in retinal neuroprotection. *Curr Opin Ophthalmol.* 2014;25:228–233.
- Krishnan A, Fei F, Jones A, et al. Overexpression of soluble Fas ligand following Adeno-associated virus gene therapy prevents retinal ganglion cell death in chronic and acute murine models of glaucoma. *J Immunol.* 2016;197:4626–4638.
- Besirli CG, Chinskey ND, Zheng QD, Zacks DN. Inhibition of retinal detachment-induced apoptosis in photoreceptors by a small peptide inhibitor of the fas receptor. *Invest Ophthalmol Vis Sci.* 2009;51:2177–2184.
- Zacks DN, Hanninen V, Pantcheva M, Ezra E, Grosskreutz C, Miller JW. Caspase activation in an experimental model of retinal detachment. *Invest Ophthalmol Vis Sci.* 2003;44:1262–1267.
- Zacks DN, Zheng QD, Han Y, Bakhru R, Miller JW. FAS-mediated apoptosis and its relation to intrinsic pathway activation in an experimental model of retinal detachment. *Invest Ophthalmol Vis Sci.* 2004;45:4563–4569.
- Kim Y, Tarallo V, Kerur N, et al. DICER1/*Alu* RNA dysmetabolism induces Caspase-8-mediated cell death in age-related macular degeneration. *Proc Natl Acad Sci USA.* 2014;111:16082–16087.
- Dunaief JL, Dentchev T, Ying GS, Milam AH. The role of apoptosis in age-related macular degeneration. *Arch Ophthalmol.* 2002;120:1435–1442.
- Jiang S, Moriarty-Craige SE, Li C, et al. Associations of plasma-soluble fas ligand with aging and age-related macular degeneration. *Invest Ophthalmol Vis Sci.* 2008;28:1345–1349.
- Zacks DN, Kocab AJ, Choi JJ, Gregory-Ksander MS, Cano M, Handa JT. Cell Death in AMD: The Rationale for Targeting Fas. *Clin Med.* 2022;11(3):592.
- Murakami Y, Notomi S, Hisatomi T, et al. Photoreceptor cell death and rescue in retinal detachment and degenerations. *Prog Retin Eye Res.* 2013;37:114–140.
- Krishnan A, Kocab AJ, Zacks DN, Marshak-Rothstein A, Gregory-Ksander M. A small peptide antagonist of the Fas receptor inhibits neuroinflammation and prevents axon degeneration and retinal ganglion cell death in an inducible mouse model of glaucoma. *J Neuroinflammation.* 2019;16:184.
- Xiao J, Yao J, Jia L, Lin C, Zacks DN. Protective effect of Met12, a small peptide inhibitor of Fas, on the retinal pigment epithelium and photoreceptor after sodium iodate injury. *Invest Ophthalmol Vis Sci.* 2017;58:1801–1810.
- Huckfeldt RM, Vavvas DG. Neuroprotection for retinal detachment. *Int Ophthalmol Clin.* 2013;53:105–117.
- Lee ES, Flannery JG. Transport of Truncated Rhodopsin and Its Effects on Rod Function and Degeneration. *Invest Ophthalmol Vis Sci.* 2007;48(6):2868–2876.
- Dryja TP, McGee TL, Hahn LB, et al. Mutations within the rhodopsin gene in patients with autosomal dominant retinitis pigmentosa. *N Engl J Med.* 1990;323(19):1302–1307.
- Dryja TP, Hahn LB, Cowley GS, McGee TL, Berson EL. Mutation spectrum of the rhodopsin gene among patients with autosomal dominant retinitis pigmentosa. *Proc Natl Acad Sci USA.* 1991;88(20):9370–9374.
- Daiger SP, Bowne SJ, Sullivan LS. Perspective on genes and mutations causing retinitis pigmentosa. *Arch Ophthalmol.* 2007;125:151–158.
- Jensen R. Differential effects of antipsychotic drugs on contrast response functions of retinal ganglion cells in wild-type Sprague-Dawley rats and P23H retinitis pigmentosa rats. *PLoS One.* 2019;14:e0218200.
- Perdices L, Fuentes-Broto L, Segura F, et al. Hepatic oxidative stress in pigmented P23H rhodopsin transgenic rats with progressive retinal degeneration. *Free Radic Biol Med.* 2018;124:550–557.
- Lowe RJ, Daniello KM, Duncan JL, et al. Influence of eye pigmentation on retinal degeneration in P23H and S334ter mutant rhodopsin transgenic rats. *Exp Eye Res.* 2019;187:107755.
- Sizova OS, Shinde VM, Lenox AR, Gorbatyuk MS. Modulation of cellular signaling pathways in P23H rhodopsin photoreceptors. *Cell Signal.* 2014;26:665–672.
- Comitato A, Di Salvo MT, Turchiano G, et al. Dominant and recessive mutations in rhodopsin activate different cell death pathways. *Hum Mol Genet.* 2016;25:2801–2812.
- Viringipurampeer IA, Metcalfe AL, Bashar AE, et al. NLRP3 inflammasome activation drives bystander cone photoreceptor cell death in a P23H rhodopsin model of retinal degeneration. *Hum Mol Genet.* 2016;25:1501–1516.
- Yao J, Qiu Y, Frontera E, et al. Inhibiting autophagy reduces retinal degeneration caused by protein misfolding. *Autophagy.* 2018;14(7):1226–1238.
- Qiu Y, Yao J, Jia L, Thompson DA, Zacks DN. Shifting the balance of autophagy and proteasome activation reduces proteotoxic cell death: A novel therapeutic approach for restoring photoreceptor homeostasis. *Cell Death Dis.* 2019;10:547.
- Noorwez SM, Kuksa V, Imanishi Y, et al. Pharmacological chaperone-mediated in vivo folding and stabilization of the P23H-opsin mutant associated with autosomal dominant retinitis pigmentosa. *J Biol Chem.* 2003;278:14442–14450.
- Kaushal S, Khorana HG. Structure and function in rhodopsin. Point mutations associated with autosomal dominant retinitis pigmentosa. *Biochem.* 1994;33:6121–6128.
- Illing ME, Rajan RS, Bence NF, Kopito RR. A rhodopsin mutant linked to autosomal dominant retinitis pigmentosa is prone to aggregate and interacts with the ubiquitin proteasome system. *J Biol Chem.* 2002;277:34150–34160.
- Tam BM, Moritz OL. Characterization of rhodopsin P23H-induced retinal degeneration in a *Xenopus laevis* model of retinitis pigmentosa. *Invest Ophthalmol Vis Sci.* 2006;47:3234–3241.
- Sakami S, Maeda T, Bereta G, et al. Probing mechanisms of photoreceptor degeneration in a new mouse model of the common form of autosomal dominant retinitis pigmentosa due to P23H opsin mutations. *J Biol Chem.* 2011;286:10551–10567.
- Chiang WC, Kroeger H, Sakami S, et al. Robust endoplasmic reticulum-associated degradation of rhodopsin precedes retinal degeneration. *Mol Neurobiol.* 2015;52:679–695.
- Mendes HF, Cheetham ME. Pharmacological manipulation of gain-of-function and dominant-negative mechanisms in rhodopsin retinitis pigmentosa. *Hum Mol Genet.* 2008;17:3043–3054.

37. Michalakakis S, Becirovic E, Biel M. Retinal Cyclic Nucleotide-Gated Channels: From Pathophysiology to Therapy. *Int J Mol Sci.* 2018;19(3):749.
38. Olivares-González L, Velasco S, Campillo I, et al. Nutritional Supplementation Ameliorates Visual Function, Retinal Degeneration, and Redox Status in rd10 Mice. *Antioxidants (Basel).* 2021;10(7):1033.
39. Campello L, Kutsyr O, Noailles A, et al. New Nrf2-Inducer Compound ITH12674 Slows the Progression of Retinitis Pigmentosa in the Mouse Model rd10. *Cell Physiol Biochem.* 2020;54(1):142–159.
40. Nakatake S, Murakami Y, Ikeda Y, et al. MUTYH promotes oxidative microglial activation and inherited retinal degeneration. *JCI Insight.* 2016;1(15):e87781.
41. Pang J, Dai X, Boye SE, et al. Long-term Retinal Function and Structure Rescue Using Capsid Mutant AAV8 Vector in the rd10 Mouse, a Model of Recessive Retinitis Pigmentosa. *Mol Ther.* 2011;2:234–242.
42. McLaughlin ME, Ehrhart TL, Berson EL, Dryja TP. Mutation spectrum of the gene encoding the  $\beta$  subunit of rod phosphodiesterase among patients with autosomal recessive retinitis pigmentosa. *Proc Natl Acad Sci USA.* 1995;92:3249–3253.
43. Watanabe-Fukunaga R, Brannan CI, Copeland NG, Jenkins NA, Nagata S. Lymphoproliferation disorder in mice explained by defects in Fas antigen that mediates apoptosis. *Nature.* 1992;356(6367):314–317.
44. Yao J, Jia L, Feathers K, et al. Autophagy-mediated catabolism of visual transduction proteins prevents retinal degeneration. *Autophagy.* 2016;12:2439–245.
45. Chang B, Hawes NL, Hurd RE, Davisson MT, Nusinowitz S, Heckenlively JR. Retinal degeneration mutants in the mouse. *Vision Res.* 2002;42:517–525.
46. Chang B, Hawes NL, Pardue MT, et al. Two mouse retinal degenerations caused by missense mutations in the  $\beta$ -subunit of rod cGMP phosphodiesterase gene. *Vision Res.* 2007;47:624–633.
47. Gargini C, Terzibas E, Mazzoni F, Strettoi E. Retinal organization in the retinal degeneration 10 (rd10) mutant mouse: a morphological and ERG study. *J Comp Neurol.* 2007;500:222–238.
48. Canto A, Martínez-González J, Miranda M, Olivar T, Almansa I, Hernández-Rabaza V. Sulforaphane Modulates the Inflammation and Delays Neurodegeneration on a Retinitis Pigmentosa Mice Model. *Front Pharmacol.* 2022;13:811257.
49. Makabe K, Sugita S, Mandai M, Futatsugi Y, Takahashi M. Microglia dynamics in retinitis pigmentosa model: formation of fundus whitening and autofluorescence as an indicator of activity of retinal degeneration. *Sci Rep.* 2020;10:14700.
50. Yang W, Xiong G, Lin B. Cyclooxygenase-1 mediates neuroinflammation and neurotoxicity in a mouse model of retinitis pigmentosa. *J Neuroinflammation.* 2020;17:306.
51. Péquignot MO, Provost AC, Sallé S, et al. Major role of BAX in apoptosis during retinal development and in establishment of a functional postnatal retina. *Dev Dyn.* 2003;228(2):231–238.
52. Blank T, Goldmann T, Koch M, et al. Early Microglia Activation Precedes Photoreceptor Degeneration in a Mouse Model of CNGB1-Linked Retinitis Pigmentosa. *Front Immunol.* 2018;8:1930.
53. Karali M, Guadagnino I, Marrocco E, et al. AAV-miR-204 Protects from Retinal Degeneration by Attenuation of Microglia Activation and Photoreceptor Cell Death. *Mol Ther Nucleic Acids.* 2020;19:144–156.
54. Noailles A, Fernández-Sánchez L, Lax P, Cuenca N. Microglia activation in a model of retinal degeneration and TUDCA neuroprotective effects. *J Neuroinflammation.* 2014;11:186.
55. Zhou T, Huang Z, Sun X, et al. Microglia Polarization with M1/M2 Phenotype Changes in rd1 Mouse Model of Retinal Degeneration. *Front Neuroanat.* 2017;11:77.
56. Lew DS, Mazzoni F, Finnemann SC. Microglia Inhibition Delays Retinal Degeneration Due to MerTK Phagocytosis Receptor Deficiency. *Front Immunol.* 2020;11:1463.